

Human Islet Amyloid Polypeptide Oligomers Disrupt Cell Coupling, Induce Apoptosis, and Impair Insulin Secretion in Isolated Human Islets

Robert A. Ritzel,¹ Juris J. Meier,¹ Chia-Yu Lin,¹ Johannes D. Veldhuis,² and Peter C. Butler¹

Insulin secretion from the 2,000–3,000 β -cells in an islet is a highly synchronized activity with discharge of insulin in coordinate secretory bursts at approximately 4-min intervals. Insulin secretion progressively declines in type 2 diabetes and following islet transplantation. Both are characterized by the presence of islet amyloid derived from islet amyloid polypeptide (IAPP). In the present studies, we examined the action of extracellular human IAPP (h-IAPP) on morphology and function of human islets. Because oligomers of h-IAPP are known to cause membrane disruption, we questioned if application of h-IAPP oligomers to human islets would lead to disruption of islet architecture (specifically cell-to-cell adherence) and a decrease in coordinate function (e.g., increased entropy of insulin secretion and diminished coordinate secretory bursts). Both hypotheses are affirmed, leading to a novel hypothesis for impaired insulin secretion in type 2 diabetes and following islet transplantation, specifically disrupted cell-to-cell adherence in islets through the actions of membrane-disrupting IAPP oligomers. *Diabetes* 56:65–71, 2007

In health, insulin secretion is predominantly derived from discrete insulin secretory bursts occurring at ~4- to 6-min intervals (1–4). Increased insulin secretion in response to hyperglycemia is accomplished by amplification of insulin secretory burst mass (4–7). The islet of Langerhans is a complex organ consisting of ~2,000–3,000 β -cells that function as an integrated unit, illustrated by synchronized secretion of insulin in secretory bursts by single perfused islets (8,9). The synchronization of insulin secretion from β -cells within an islet is accomplished at least in part through electrical coupling. Tight gap junctions between the cell membranes of adjacent β -cells allow the propagation of cell membrane depolarization through the islet (10–12). This contributes

to the synchronization of the stimulus-secretion pathway downstream of membrane depolarization (e.g., elevation of the intracellular calcium concentration that, in turn, triggers exocytosis of primed and docked insulin secretory vesicles) (12).

Insulin secretion in response to an increased blood glucose concentration is impaired in both type 2 diabetes (13,14) and patients with type 1 diabetes following islet transplantation (15). In type 2 diabetes, the islet typically contains extracellular deposits of amyloid derived from the peptide islet amyloid polypeptide (IAPP) (16–19). Islet amyloid has also been reported in recently transplanted human islets (20,21). Human IAPP (h-IAPP) spontaneously aggregates into oligomers and then amyloid fibrils in an aqueous solution, while IAPP from rodents (r-IAPP) does not form oligomers or amyloid but remains in a monomeric form in an aqueous environment (22–26). Neither the mechanisms that prevent h-IAPP oligomerization in health nor those that allow formation of islet amyloid in type 2 diabetes and recently transplanted islets are known. Several reports suggest that h-IAPP oligomers, intermediate between h-IAPP monomers and h-IAPP-derived amyloid fibrils, may induce membrane leakage and disruption (24,26–29).

In the present studies, we sought to address the following questions: First, if h-IAPP is added to human islets in culture, is there an appreciable (morphological) effect on cell-to-cell integrity within the islet? We addressed this by use of both time-lapse video and confocal microscopy. Second, does addition of h-IAPP to human islets increase islet cell death? Third, does addition of h-IAPP to islets in culture disrupt subsequent glucose-mediated insulin secretion from these islets? Specifically, we hypothesized that h-IAPP oligomer-induced disruption of cell membranes might lead to decreased synchronization of insulin secretion with an attenuated increase in insulin pulse mass in response to an increment in glucose concentration.

From the ¹Larry Hillblom Islet Research Center, UCLA David Geffen School of Medicine, Los Angeles, California; and the ²Endocrine Division, Mayo Medical and Graduate Schools of Medicine, Mayo Clinic, Rochester, Minnesota.

Address correspondence to Peter C. Butler, Larry Hillblom Islet Research Center, UCLA David Geffen School of Medicine, 24-130 Warren Hall, 900 Veteran Ave., Los Angeles, CA 90095-7073. E-mail: pbutler@mednet.ucla.edu.

Received for publication 28 May 2006 and accepted in revised form 29 September 2006.

ApEn, approximate entropy; ELISA, enzyme-linked immunosorbent assay; h-IAPP, human IAPP; IAPP, islet amyloid polypeptide; r-IAPP, rodent IAPP; TLVM, time-lapse video microscopy; TUNEL, terminal deoxynucleotidyl transferase-mediated dUTP nick-end labeling.

DOI: 10.2337/db06-0734

© 2007 by the American Diabetes Association.

The costs of publication of this article were defrayed in part by the payment of page charges. This article must therefore be hereby marked "advertisement" in accordance with 18 U.S.C. Section 1734 solely to indicate this fact.

RESEARCH DESIGN AND METHODS

Human pancreatic islets were incubated for 48 h in Click's culture medium at 5 mmol/l glucose containing vehicle (water with 0.5% acetic acid), r-IAPP (40 μ m), or h-IAPP (40 μ m). Human and rat IAPP were purchased from Bachem California (Torrance, CA). During static incubation, human islets were studied with time-lapse video microscopy (TLVM). After static incubation, the islets were either analyzed with confocal microscopy, stained using the TUNEL (terminal deoxynucleotidyl transferase-mediated dUTP nick-end labeling) method to detect islet cells undergoing apoptosis, or studied in perfusion experiments.

Islet culture. Islets from the pancreas of eight nondiabetic heart-beating organ donors (five males, three females, age 39 ± 12 years, BMI 26.1 ± 5.4 kg/m², islet purity $88 \pm 7\%$, islet viability $93 \pm 3\%$) were isolated in the Northwest Tissue Center, Seattle (R. Paul Robertson), and the University of

Minnesota Diabetes Institute for Immunology and Transplantation (Bernhard J. Hering). The islets were maintained in RPMI culture medium with 5 mmol/l glucose and 10% fetal bovine serum at 37°C in humidified air containing 5% CO₂. Experiments were performed in random order after a minimum recovery period of 4 days following the islet isolation process.

TLVM. TLVM is a technique that allows real-time imaging of living tissue. TLVM was performed as described previously for imaging of a β -cell line (25). Briefly, human islets were incubated in a specially prepared microculture dish (2.3 cm diameter; Bioprotechs Δ T Culture Dish, Butler, PA). The microculture dish was mounted onto the motorized stage (H107, ProScan; Prior Scientific) of an inverted microscope (Inverted System Microscope IX 70; Olympus, Melville, NY). The microculture dish was specially designed with an optically transparent, electrically conductive indium tin-oxide coating on the bottom surface to provide direct heat transfer to cells. The temperature inside the dish was dynamically controlled to $37 \pm 0.1^\circ\text{C}$ (Δ T Culture Dish Controller, Bioprotechs). The dish was covered with an electrically heated, optically transparent lid to prevent condensation from forming on the under surface of the cover. pH was stabilized by the inflow of air containing 5% CO₂. The pH of the culture medium was recorded in separate experiments with a pH microelectrode (PHR-146; Lazar Research Laboratories, Los Angeles, CA) and remained stable throughout the 48-h observation period. Images of incubated islets were acquired with an analog camera (3-CCD camera; Optronics) every 10 min and stored and analyzed on a personal computer (Intel Pentium processor, 700 MHz; Image-Pro Plus and Scope Pro software). To analyze the impact of h-IAPP on islet morphology and integrity, we measured the islet cross-sectional area of human islets in 4-h intervals during the full experimental period. The results are expressed as changes in islet cross-sectional area in μm^2 as a function of time.

TUNEL staining. The number of apoptotic cells in human islets after 48 h of static incubation was detected using the TUNEL method (In Situ Cell Death Detection Kit, AP; Roche Diagnostics, Indianapolis, IN). After staining, the number of TUNEL-positive cells per islet was determined using an inverted microscope (Inverted System Microscope IX 70), as described previously (25,30). Briefly, TUNEL-positive cells were counted, while stained debris, which was occasionally present, was not included. The results are expressed as number of TUNEL-positive cells per mean islet cross-sectional area of the group to account for different sizes of individual islets. At the beginning of the experiments, there was no difference in the mean islet cross-sectional area between the groups ($P = \text{NS}$).

Immunofluorescent staining for insulin and TUNEL. Human islets were cultured with h-IAPP and vehicle control as described above. Then islets were washed with PBS and fixed in 4% paraformaldehyde at 4°C overnight. The islets were resuspended in Histogel (Richard-Allan Scientific, Kalamazoo, MI) followed by a rapid centrifugation and paraffin embedding. Sections were defatified in toluene, rehydrated in grades of alcohol, and washed in H₂O followed by proteinase K treatment for 15 min at 37°C. Human islets were stained with TUNEL by cell death detection kit (TMR Red; Roche Diagnostics, Mannheim, Germany) and then costained with insulin (Guinea Pig Anti-Insulin Ab; Zymed Laboratories, South San Francisco, CA), 1:100 dilution at 4°C overnight followed by FITC donkey anti-guinea pig (Jackson ImmunoResearch Laboratories, West Grove, PA), 1:200 dilution for 1 h at room temperature. Slides were mounted with Vectashield (Vector Laboratories, Burlingame, CA) with DAPI. Fluorescent slides were viewed using a Leica DM6000 microscope (Leica Microsystems, Bannockburn, IL) and images acquired by Openlab software (Improvision, Lexington, MA).

Confocal microscopy. Human islet and islet cell morphology were determined with confocal microscopy. After 48 h of static incubation with and without IAPP, human islets were stained for 1 h at 37°C in a humidified atmosphere with 10 $\mu\text{mol/l}$ DiI (1,1'-dioctadecyl-3,3',3'-tetramethylindocarbocyanine perchlorate; Molecular Probes, Eugene, OR). The islets were then washed and incubated for 10 min with cold PBS (4°C). Fixation was subsequently performed with paraformaldehyde 1% for 10 min at room temperature. Imaging was performed in the Imaging Core of the Doheny Eye Institute at the University of Southern California, Los Angeles, using a helium-neon laser for excitation (543 nm) and a Rhodamine narrow band filter. Confocal images of human islets were analyzed on a personal computer (Intel Pentium processor, 700 MHz; Image-Pro Plus and Scope Pro software). DiI is a lipophilic dye that incorporates into membranes and diffuses laterally resulting in staining of the entire cell. The images allow resolution of single islet cells for the measurement of islet cell cross-sectional area. This analysis was performed by outlining single cells and subsequent computation of this area. To assess whether h-IAPP disrupts cell-to-cell adhesions, we measured the distance between the unstained nuclei of neighboring cells. Occasionally there was irregular stained material inside islets without a discernable cellular structure (Fig. 5A). The distances between cells across this stained material were not included in this analysis.

Islet perfusion. For the analysis of human islet function after static incubation with ($n = 6$ runs) and without h-IAPP ($n = 7$ runs), islets were studied in an islet perfusion system, which has previously been described in detail and validated for quantification of pulsatile insulin release from human islets (31). Immediately following static incubation, aliquots of human islets were suspended in Bio-Gel P-2 beads (Bio-Rad, Hercules, CA) and placed in perfusion chambers (10–15 islets per chamber). The perfusion system (ACUSYST-S; Cellex Biosciences, Minneapolis, MN) consisted of a multi-run peristaltic pump that delivered perfusate through three to four parallel tubing sets via a heat exchanger and perfusion chambers at a constant rate of 0.3 ml/min. The perfusion buffers (Krebs-Ringer bicarbonate [KRB] buffer: NaCl 115 mmol/l, KCl 4.7 mmol/l, CaCl₂ 2.5 mmol/l, MgCl₂ 1.2 mmol/l, NaHCO₃ 5 mmol/l, pH 7.4) were supplemented with 0.2% human serum albumin, prewarmed to 37°C, and oxygenized with 95% O₂ and 5% CO₂. The perfusate (4 mmol/l glucose) was delivered to the perfusion chambers containing the human islets and, after an equilibration period of 40 min, the effluent was collected in 1-min intervals over 100 min.

At 40 min, the glucose concentration in the perfusion buffer was increased to 16 mmol/l. Before and after perfusion, the diameters of human islets were measured to account for different human islet sizes. After perfusion, the islets were retrieved from the chambers and processed for the determination of islet insulin content. To accomplish this, the islets were washed in RPMI 1640 and lysed with 600 μl ice-cold lysis buffer [50 mmol/l HEPES, 0.1% (vol/vol) Triton X-100, 1 $\mu\text{mol/l}$ phenylmethylsulfonyl fluoride, 10 $\mu\text{mol/l}$ E-64, 10 $\mu\text{mol/l}$ pepstatin A, 10 $\mu\text{mol/l}$ tosyl-Lys-chloromethyl ketone, 100 $\mu\text{mol/l}$ leupeptin (pH 8.0)]. After sonication (25 W for 40 s) and centrifugation (12,000g for 5 min), the resultant supernatants were stored at -20°C and subsequently analyzed for insulin concentration and, thus, islet insulin content.

Laboratory determinations. Glucose concentrations in the perfusion buffers and in the culture media were measured with the glucose oxidase method (Glucose Analyzer 2; Beckman Instruments, Brea, CA). Insulin was measured in duplicate with a two-site immunospecific enzyme-linked immunosorbent assay (ELISA) as previously described (32). There is no cross-reactivity with proinsulin and split 32,33 and 31,32 proinsulins. The lower detection limit is ~ 4 pmol/l and the assay range is 4–2,000 pmol/l. The intra-assay coefficient of variation ranged from 1.7 to 3.2%. The interassay coefficient of variation ranged from 3.5 to 4.5%.

Calculations and statistical analysis. Insulin secretion during islet perfusion is expressed in mass units per islet per minute. The insulin concentration time series were analyzed by deconvolution to quantify insulin secretion dynamics. Deconvolution analysis is a multiparameter technique to detect and quantify insulin secretory bursts as described previously. Deconvolution analysis has been specifically validated for this perfusion system (31). Briefly, deconvolution analysis computes the insulin secretion rate from the insulin concentration time profile while identifying the position, duration, mass, and amplitude of insulin secretory bursts within this secretion profile. These calculations are possible because of the known half-life for the hormone in this perfusion system (0.63 min).

The regularity or orderliness of insulin secretion from human islets in perfusion was analyzed with approximate entropy (ApEn). ApEn is a model-independent and scale-invariant statistic designed to quantify the regularity or orderliness of (hormone) time series (33). Technically, ApEn measures the logarithmic likelihood that runs of patterns that are close (within r) for m contiguous observations remain close (within the tolerance width r) on subsequent incremental comparisons. This regularity metric is validated for parameter choices of $r = 0.2 \times \text{SD}$ in the individual time series and $m = 1$, as used here (34–36). Larger ApEn values indicate a higher degree of process randomness. A precise mathematical definition is given by Pincus (33).

ANOVA and Student's t test were used to test human islet cross-sectional areas, insulin secretion data, parameters of insulin pulsatility, islet cell cross-sectional areas, and islet internuclei distances for statistical significance. A P value of < 0.05 was considered to denote significant differences.

RESULTS

TLVM. Human islets were imaged during static incubation with TLVM to study the impact of h-IAPP on islet architecture. Incubation with 40 $\mu\text{mol/l}$ h-IAPP for 48 h resulted in an $\sim 20\%$ increase of the islet cross-sectional area (Figs. 1 and 2), whereas static incubation without h-IAPP did not change the islet cross-sectional area ($P = \text{NS}$). TLVM also reveals that during incubation with h-IAPP, single islet cells repeatedly appeared at the islet surface, leading to disintegration of the islet structure and thereby contributing to the expansion of the islet cross-sectional area (Fig.

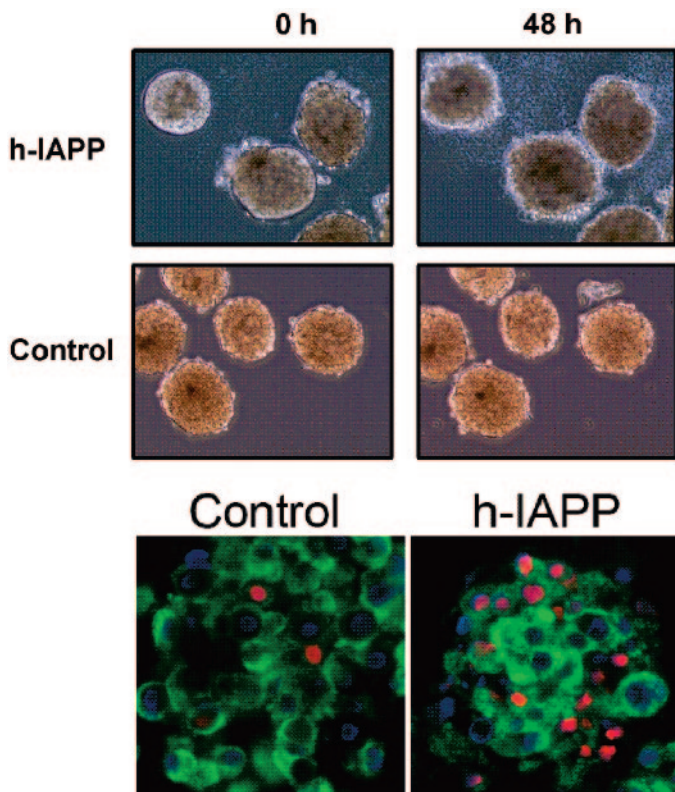


FIG. 1. *Upper panels:* Brightfield microscopic images (magnification $\times 100$) of isolated islets in culture from nondiabetic human subjects before and after 48 h of incubation with and without h-IAPP (40 $\mu\text{mol/l}$). Note the expansion of the islet cross-sectional area and disintegration of the islet shape if islets were incubated with h-IAPP versus control. *Lower panels:* Representative immunofluorescent images of human islets ($n = 120$ and $n = 125$ for control and h-IAPP, respectively) similarly treated as above but subsequently fixed and immunostained for insulin (green) and apoptosis by TUNEL (red). Fixation and dehydration distorts islet architecture but increased apoptosis of β -cells and other cells types after exposure to h-IAPP is apparent.

3). Some of the cells, which appeared at the islet surface, exhibited morphological changes characteristic of apoptosis: cell shrinkage, fragmentation, and development of an apoptotic halo (Fig. 3).

TUNEL staining of human islets. To confirm that under the present experimental conditions h-IAPP induces

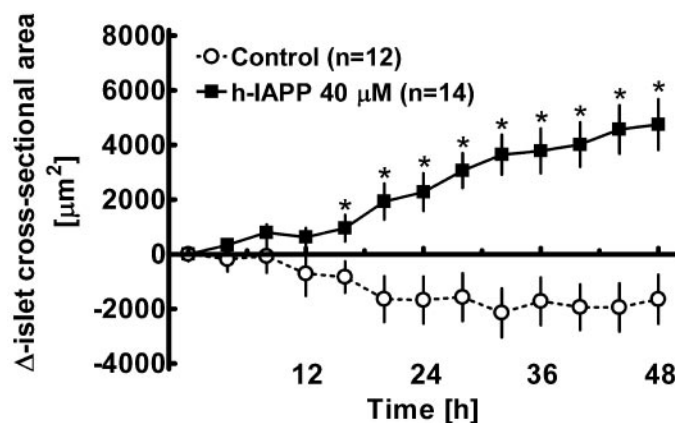


FIG. 2. Change of the islet cross-sectional area during 48 h of incubation with h-IAPP versus control. $P < 0.0001$ by repeated-measures ANOVA. Data are means \pm SEM. * $P < 0.05$ for differences versus control at individual time points (one-way ANOVA).

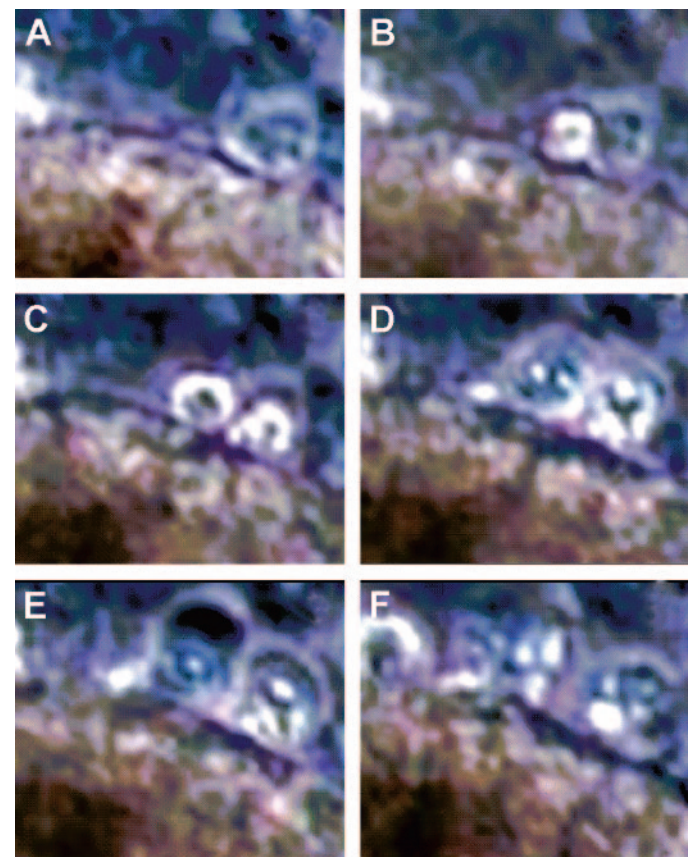


FIG. 3. Sections ($10\times$ zoom) from microscopic images (magnification $100\times$) of an isolated islet from a nondiabetic human subject. Images were acquired during 48 h of incubation with h-IAPP (40 $\mu\text{mol/l}$). The time interval between individual images is 20 min, starting at 15 h of incubation (A). A–F: Two cells appear at the islet surface and subsequently display morphological changes characteristic of apoptosis: cell shrinkage, fragmentation, and development of an apoptotic halo.

apoptosis in isolated human islets, after static incubation the islets were fixed and apoptotic cells detected with the TUNEL method. After 48 h of incubation of human islets with 40 $\mu\text{mol/l}$ h-IAPP, the number of apoptotic cells per islet increased fourfold compared with control islets ($P < 0.001$; Fig. 4). Incubation of human islets with nonamyloidogenic r-IAPP did not induce apoptosis in isolated human islets (Fig. 4).

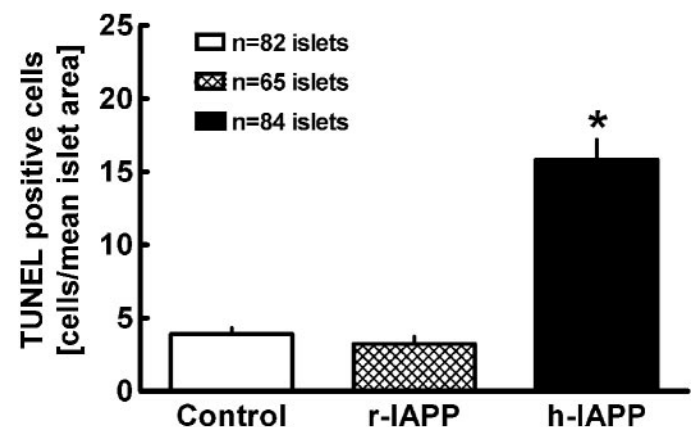


FIG. 4. Mean number of TUNEL-positive cells in human islets ($n = 3$ donors) incubated for 48 h with vehicle (control), r-IAPP (40 $\mu\text{mol/l}$), or h-IAPP (40 $\mu\text{mol/l}$). Data are means \pm SEM. * $P < 0.05$ vs. control.

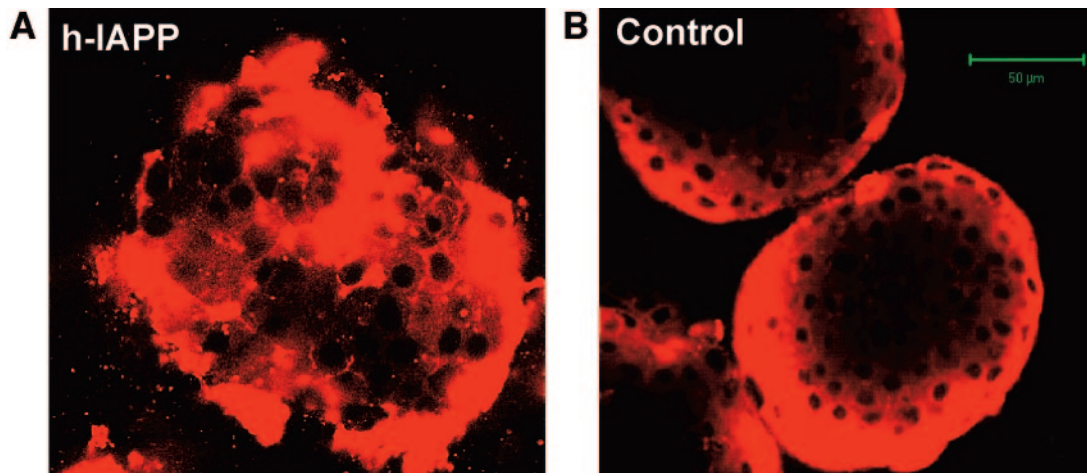


FIG. 5. Confocal micrographs showing representative human islets stained with DiI after 48 h of static incubation with 40 $\mu\text{mol/l}$ (A) or without h-IAPP (B).

In addition, to confirm human IAPP-induced β -cell apoptosis, human islets were similarly treated but after fixation stained by immunofluorescence for insulin and by the TUNEL technique as above. Islets exposed to human IAPP had a sixfold increased β -cell apoptosis ($P < 0.001$) compared with controls (Fig. 1, lower panel).

Confocal microscopy. For further characterization of the mechanism of how incubation of human islets with h-IAPP induces an increase of the islet cross-sectional area, we studied human islets with confocal microscopy. In general, an increase of the islet cross-sectional area could result from islet cell hypertrophy and/or an increase of the spatial distance between cells (loosening of islet architecture). After 48 h of static incubation without h-IAPP, the islet cells within the islets were regularly organized and immediately adjacent to each other (Fig. 5B). In contrast, if the islets had previously been incubated with h-IAPP, the organization of islet cells appeared less regular, particularly because there was irregular stained material inside and adjacent to islets, which most likely represents cellular debris from disintegrated apoptotic cells (Fig. 5A). In the present experiments with exogenous application of IAPP, this material was more likely to be found in the mantle of the islets than in the core. The analysis of the cross-sectional area of intact islet cells was performed by outlining single cells and subsequent calculation of their area. There was no difference in the cell size after incubation with h-IAPP compared with control experiments ($P = \text{NS}$; Fig. 6A). However, incubation with h-IAPP induced a significant increase of the internucleus distance between islet cells (Fig. 6B). The histogram of the internucleus distances reveals that the increase was due to an access in the range of $\sim 6 \mu\text{m}$ (Fig. 6C). These results suggest that incubation of isolated human islets with h-IAPP might lead to not only islet cell apoptosis, but also to a partial structural disruption of cell-to-cell adhesions with increased spatial distance between islet cells.

Islet perfusion. After 48 h of static incubation, human islet function was evaluated in islet perfusion experiments (Fig. 7). Insulin secretion, for islets cultured under control conditions or with h-IAPP, exhibited a pulsatile pattern (Fig. 7). The pulse interval of pulsatile insulin secretion was robust to glucose stimulation in both exper-

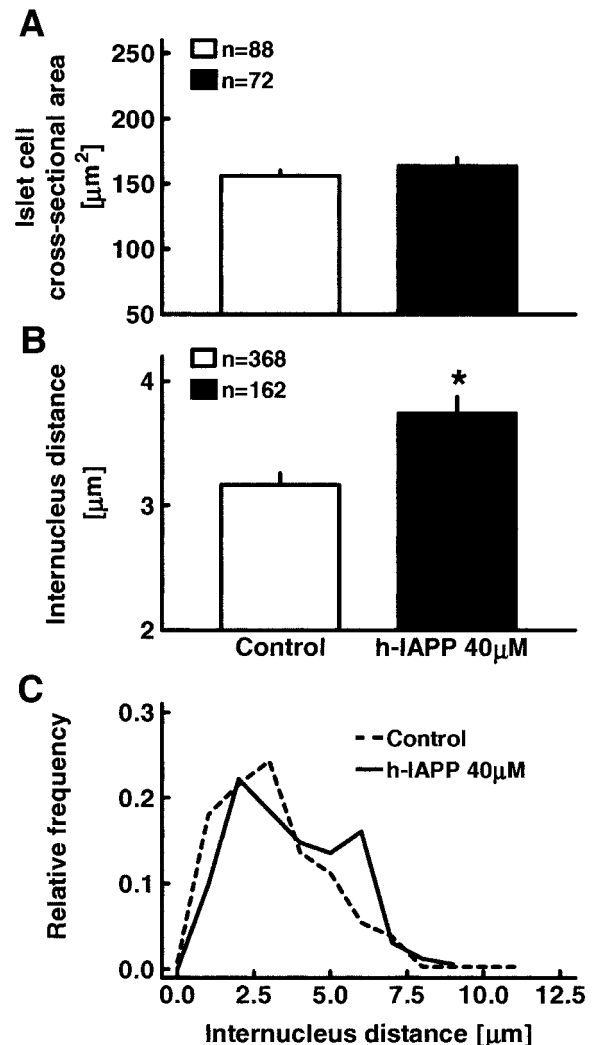


FIG. 6. Islet cell cross-sectional area (A) and internucleus distance (B) in isolated human islets after 48 h of static incubation with and without h-IAPP. C: Relative frequency distribution of the internucleus distance in human islets after 48 h of incubation with and without h-IAPP. For A and B, data are means \pm SEM. * $P < 0.05$ vs. control.

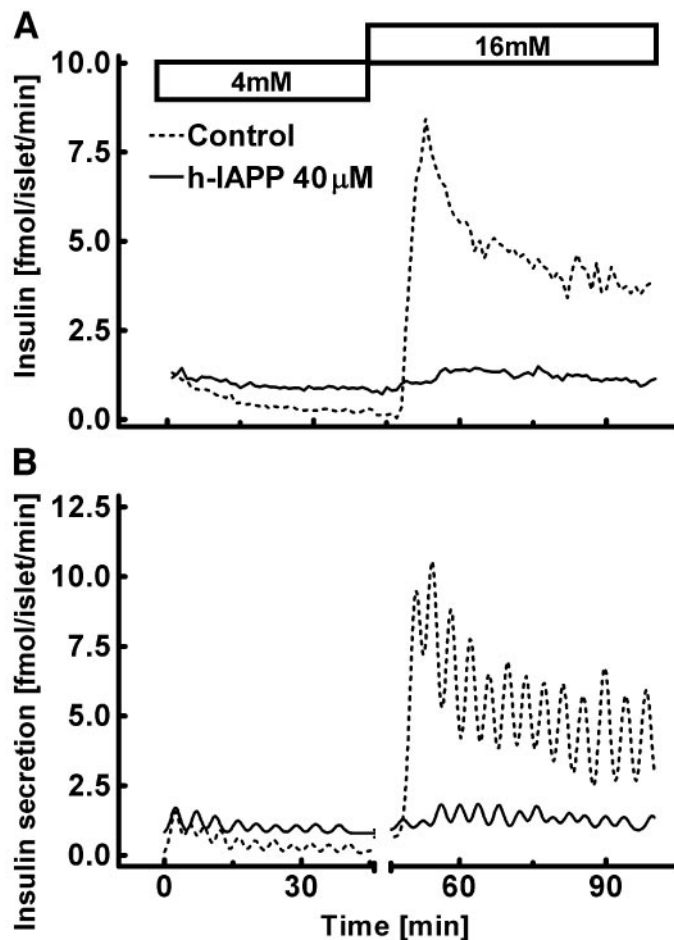


FIG. 7. Insulin profiles (A) and insulin secretion rates (derived by deconvolution analysis) (B) from two representative islet perfusion experiments performed after 48 h of static incubation with and without h-IAPP. Islets were maintained at 4 mmol/l glucose from 0 to 40 min and at 16 mmol/l glucose from 40 to 100 min.

imental groups (Fig. 8) ($P = \text{NS}$ for comparison of control vs. h-IAPP and 4 vs. 16 mmol/l glucose). Elevation of glucose concentrations in the perfusate to 16 mmol/l induced a large amplitude early-secretory response followed by a period of insulin secretion characterized by smaller secretion amplitudes (Fig. 7), which lasted until the end of the perfusion experiment. Prior incubation of human islets with h-IAPP diminished mean insulin secretion at 4 mmol/l glucose by $\sim 50\%$ (0.8 ± 0.1 vs. 0.4 ± 0.2 fmol \cdot islet $^{-1} \cdot$ min $^{-1}$; $P = 0.04$, control vs. h-IAPP) and at 16 mmol/l glucose by $\sim 90\%$ (2.8 ± 0.4 vs. 0.3 ± 0.2 fmol \cdot islet $^{-1} \cdot$ min $^{-1}$; $P < 0.001$, control vs. h-IAPP). In three channels of six runs with islets previously incubated with h-IAPP, insulin secretion was sometimes undetectable with the present ELISA; these runs could not be analyzed by deconvolution and ApEn. The functional defect to respond to glucose stimulation was due to $\sim 50\%$ and $\sim 80\%$ deficits in insulin pulse mass (Fig. 8) at 4 and 16 mmol/l glucose, respectively. The islet insulin content of islets cultured with h-IAPP was reduced by $\sim 60\%$ compared with control ($1,162 \pm 260$ vs. $2,915 \pm 524$ fmol/islet; $P = 0.02$).

Raw insulin secretion data from perfusion experiments were further analyzed by ApEn to assess whether incubation with h-IAPP has functional implications for the regularity or orderliness of insulin secretion from isolated

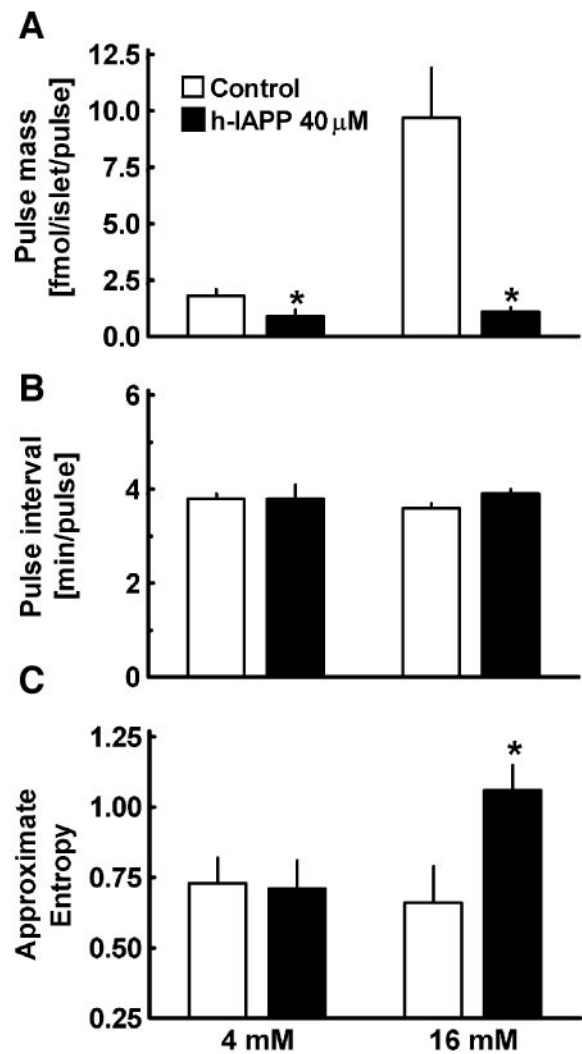


FIG. 8. Mean pulse mass (A), pulse interval (B), and ApEn (C) during perfusion of human islets at 4 mmol/l and 16 mmol/l glucose ($n = 4$ runs for control and $n = 3$ runs for h-IAPP) after 48 h of static incubation with and without h-IAPP. Following incubation with h-IAPP, insulin was undetectable in the effluent of two runs by ELISA. Data are means \pm SEM. * $P < 0.05$ vs. control.

human islets. The orderliness of insulin secretion was not affected by prior culture with h-IAPP during perfusion at 4 mmol/l glucose. In contrast, when human islets were stimulated with 16 mmol/l glucose, insulin secretion was significantly more disorderly than in control islets (Fig. 8).

DISCUSSION

We report that exposure of human islets to h-IAPP disrupts islet morphology and glucose-mediated insulin secretion. Human islets in static incubation with h-IAPP increased in size when examined over a 48-h period by repeated imaging despite shedding cells from the periphery of the islet. This increase in size was consistent with our posed hypothesis that h-IAPP oligomers would disrupt cell-to-cell contact through the documented adverse effects of h-IAPP oligomers on cell membranes. However, it is possible that the increased size of human islets exposed to h-IAPP was due to an increase in the size of the constituent cells. We excluded this by confocal microscopy and documented the appearance of abnormal spaces between cells after exposure of islets to h-IAPP. Both

disruption of cell membranes and induction of cell death by addition of amyloidogenic proteins are mediated by small oligomeric forms of these proteins that are distinct from amyloid fibrils (24,26). The fact that we observe increased islet cell apoptosis together with disruption of cell-to-cell integrity in these studies implies that such h-IAPP oligomers were formed under the present experimental conditions. It is unknown if the extracellular amyloid present in type 2 diabetes (16–19) or after islet transplantation (20,21) forms intracellularly and/or extracellularly and whether the h-IAPP oligomers intermediate from h-IAPP monomers and h-IAPP fibrils are the same h-IAPP oligomers that cause membrane disruption.

Indeed, because the simple addition of h-IAPP to islets causes cell-to-cell disruption, it might be questioned, what are the mechanisms present in healthy islets that prevent recently secreted h-IAPP from forming toxic oligomers? One possible factor is the associated high insulin content discharged from the insulin secretory vesicle since insulin inhibits h-IAPP amyloid formation in an aqueous environment (37). Also, the acidic pH in the secretory vesicle may be sufficient in the immediate site of exocytosis to prevent h-IAPP oligomerization (38). It is not yet technically feasible to directly address these mechanisms. From a clinical perspective, the pressing question is whether the disruption of cell-to-cell membrane interaction by h-IAPP oligomers impacts insulin secretion.

In the present studies, culture of human islets with h-IAPP had a profound adverse effect on subsequent glucose-mediated insulin secretion. One explanation is simply a reduction in the number of β -cells through the mechanisms of increased islet cell apoptosis caused by the actions of h-IAPP oligomers after addition of h-IAPP. Although this explanation might account for the decrease in glucose-induced insulin secretion, the extent of islet cell loss over the time period from addition of h-IAPP to the end of the study was insufficient to be measurable by quantitative analysis (and certainly less than the ~90% decrease in glucose-induced insulin secretion). An alternative explanation is the action of IAPP through its cell surface receptor to inhibit insulin secretion (39). However, any receptor-mediated actions of IAPP would be most evident with r-IAPP that would have remained monomeric in conditions of culture, in contrast to h-IAPP that would have spontaneously formed h-IAPP oligomers. However, using human islets previously cultured with nonamyloidogenic r-IAPP in two islet perfusion runs, we did not observe a deficit in mean insulin secretion (data not shown). Also, under conditions of perfusion, almost no h-IAPP in solution would remain given the high flow rate and resulting dilution. It is therefore unlikely that the deficient glucose-mediated insulin secretion present in islets cultured with h-IAPP was a consequence of the physiological actions of IAPP.

Prior studies have shown that glucose-mediated insulin secretion is decreased in single β -cells compared with those operating in electrically coupled groups of cells (40,41). To explore our postulate that decreased insulin secretion in islets exposed to h-IAPP oligomers is at least in part a consequence of disrupted cell-to-cell integration within the islet, we used the statistic approximate entropy (ApEn). The degree of orderliness of neuroendocrine secretion is a measure of the number of inputs that impact this secretion. Recently we reported that glucose acts as a coordinating trigger to enhance the orderliness of insulin secretion from human isolated human islets (4). The

higher the degree of synchrony between the cells within an islet, the higher the degree of orderliness of insulin secretion can be anticipated. Conversely, entropy (the inverse of orderliness) would be expected to decrease with coordinate action of β -cells within the multicellular islet organelle. Here we report a marked decrease in orderliness (increased entropy) of insulin secretion by islets exposed to h-IAPP, strongly supporting the loss of synchrony between β -cells. This is further supported by the loss of glucose-induced insulin secretion and, in particular, insulin secretory burst mass predictable by loss of synchrony between β -cells within islets. Interestingly, it has been reported that entropy of glucose-mediated insulin secretion is increased in patients with type 2 diabetes (42), but this has not been measured following islet transplantation.

The present study has the limitation that it has been carried out within isolated islets in culture. Islet isolation itself induces physical, chemical, and anoxic stresses on islets due to the loss of islet blood supply and enzyme digestion. Moreover, in addition to losing blood supply, isolated islets in culture rapidly lose vascular endothelial cells and the matrix that they may provide, as well as islet innervation and any paracrine signals arising from surrounding exocrine tissue. However, in prior studies, we were able to show that despite these limitations, the primary functional measures evaluated in the present studies (pulsatile insulin secretion in relation to glucose stimulation) are retained in isolated islets (4). Moreover, the comparison made here is between islets exposed to h-IAPP and those exposed to r-IAPP, so that differences between insulin secretion by these islets should reflect this treatment rather than conditions of islet isolation. It is of course impossible to be certain that these observed differences would also be present in the same islets in vivo.

In conclusion, the present experiments provide evidence that h-IAPP oligomers may act through their known membrane effects to disturb cell-to-cell integrity within human islets. These actions of h-IAPP, in combination with its β -cell toxic effect, severely impair subsequent glucose-mediated insulin secretion. Specifically, we have shown a reduction of insulin pulse mass accompanied by an increase in entropy of pulsatile insulin secretion, implying a loss of cell-to-cell synchronization within the islet. These mechanisms might contribute to impaired islet function in type 2 diabetes and following islet transplantation.

REFERENCES

1. Porksen N, Nyholm B, Veldhuis JD, Butler PC, Schmitz O: In humans at least 75% of insulin secretion arises from punctuated insulin secretory bursts. *Am J Physiol* 273:E908–E914, 1997
2. Song SH, McIntyre SS, Shah H, Veldhuis JD, Hayes PC, Butler PC: Direct measurement of pulsatile insulin secretion from the portal vein in human subjects. *J Clin Endocrinol Metab* 85:4491–4499, 2000
3. Porksen N, Grofte T, Greisen J, Mengel A, Juhl C, Veldhuis JD, Schmitz O, Rossle M, Vilstrup H: Human insulin release processes measured by intraportal sampling. *Am J Physiol* 282:E695–E702, 2002
4. Ritzel RA, Veldhuis JD, Butler PC: Glucose stimulates pulsatile insulin secretion from human pancreatic islets by increasing secretory burst mass: dose-response relationships. *J Clin Endocrinol Metab* 88:742–747, 2003
5. Chou HF, Ipp E: Pulsatile insulin secretion in isolated rat islets. *Diabetes* 39:112–117, 1990
6. Porksen N, Munn S, Steers J, Veldhuis JD, Butler PC: Effects of glucose ingestion versus infusion on pulsatile insulin secretion: the incretin effect is achieved by amplification of insulin secretory burst mass. *Diabetes* 45:1317–1323, 1996
7. Bergsten P: Glucose-induced pulsatile insulin release from single islets at stable and oscillatory cytoplasmic Ca^{2+} . *Am J Physiol* 274:E796–E800, 1998

8. Marchetti P, Scharp DW, McLear M, Gingerich R, Finke E, Olack B, Swanson C, Giannarelli R, Navalesi R, Lacy PE: Pulsatile insulin secretion from isolated human pancreatic islets. *Diabetes* 43:827–830, 1994
9. Lin JM, Fabregat ME, Gomis R, Bergsten P: Pulsatile insulin release from islets isolated from three subjects with type 2 diabetes. *Diabetes* 51:988–993, 2002
10. Eddlestone GT, Goncalves A, Bangham JA, Rojas E: Electrical coupling between cells in islets of Langerhans from mouse. *J Membr Biol* 77:1–14, 1984
11. Moreno AP, Berthoud VM, Perez-Palacios G, Perez-Armendariz EM: Biophysical evidence that connexin-36 forms functional gap junction channels between pancreatic mouse beta-cells. *Am J Physiol Endocrinol Metab* 288:E948–E956, 2005
12. Michon L, Nlend Nlend R, Bavamian S, Bischoff L, Boucard N, Caille D, Cancela J, Charollais A, Charpantier E, Klee P, Peyrou M, Populaire C, Zuilianello L, Meda P: Involvement of gap junctional communication in secretion. *Biochim Biophys Acta* 1719:82–101, 2005
13. Pfeifer MA, Halter JB, Porte D Jr: Insulin secretion in diabetes mellitus. *Am J Med* 70:579–588, 1981
14. Porte D Jr: Banting Lecture 1990: β -Cells in type II diabetes mellitus. *Diabetes* 40:166–180, 1991
15. Ryan EA, Paty BW, Senior PA, Bigam D, Alfadhli E, Kneteman NM, Lakey JR, Shapiro AM: Five-year follow-up after clinical islet transplantation. *Diabetes* 54:2060–2069, 2005
16. Maloy AL, Longnecker DS, Greenberg ER: The relation of islet amyloid to the clinical type of diabetes. *Hum Pathol* 12:917–922, 1981
17. Clark A, Cooper GJ, Lewis CE, Morris JF, Willis AC, Reid KB, Turner RC: Islet amyloid formed from diabetes-associated peptide may be pathogenic in type-2 diabetes. *Lancet* 2:231–234, 1987
18. Cooper GJ, Willis AC, Clark A, Turner RC, Sim RB, Reid KB: Purification and characterization of a peptide from amyloid-rich pancreases of type 2 diabetic patients. *Proc Natl Acad Sci U S A* 84:8628–8632, 1987
19. Johnson KH, O'Brien TD, Betsholtz C, Westermark P: Islet amyloid, islet-amyloid polypeptide, and diabetes mellitus. *N Engl J Med* 321:513–518, 1989
20. Westermark P, Eizirik DL, Pipeleers DG, Hellerstrom C, Andersson A: Rapid deposition of amyloid in human islets transplanted into nude mice. *Diabetologia* 38:543–549, 1995
21. Westermark P, Andersson A, Westermark GT: Is aggregated IAPP a cause of beta-cell failure in transplanted human pancreatic islets? *Curr Diab Rep* 5:184–188, 2005
22. Betsholtz C, Christmansson L, Engstrom U, Rorsman F, Svensson V, Johnson KH, Westermark P: Sequence divergence in a specific region of islet amyloid polypeptide (IAPP) explains differences in islet amyloid formation between species. *FEBS Lett* 251:261–264, 1989
23. Lorenzo A, Razzaboni B, Weir GC, Yankner BA: Pancreatic islet cell toxicity of amylin associated with type-2 diabetes mellitus. *Nature* 368:756–760, 1994
24. Janson J, Ashley RH, Harrison D, McIntyre S, Butler PC: The mechanism of islet amyloid polypeptide toxicity is membrane disruption by intermediate-sized toxic amyloid particles. *Diabetes* 48:491–498, 1999
25. Ritzel RA, Butler PC: Replication increases β -cell vulnerability to human islet amyloid polypeptide-induced apoptosis. *Diabetes* 52:1701–1708, 2003
26. Kaye R, Head E, Thompson JL, McIntire TM, Milton SC, Cotman CW, Glabe CG: Common structure of soluble amyloid oligomers implies common mechanism of pathogenesis. *Science* 300:486–489, 2003
27. Mirzabekov TA, Lin MC, Kagan BL: Pore formation by the cytotoxic islet amyloid peptide amylin. *J Biol Chem* 271:1988–1992, 1996
28. Anguiano M, Nowak RJ, Lansbury PT Jr: Protofibrillar islet amyloid polypeptide permeabilizes synthetic vesicles by a pore-like mechanism that may be relevant to type II diabetes. *Biochemistry* 41:11338–11343, 2002
29. Kaye R, Sokolov Y, Edmonds B, McIntire TM, Milton SC, Hall JE, Glabe CG: Permeabilization of lipid bilayers is a common conformation-dependent activity of soluble amyloid oligomers in protein misfolding diseases. *J Biol Chem* 279:46363–46366, 2004
30. Butler AE, Janson J, Bonner-Weir S, Ritzel R, Rizza RA, Butler PC: β -Cell deficit and increased β -cell apoptosis in humans with type 2 diabetes. *Diabetes* 52:102–110, 2003
31. Song SH, Kjems L, Ritzel R, McIntyre SM, Johnson ML, Veldhuis JD, Butler PC: Pulsatile insulin secretion by human pancreatic islets. *J Clin Endocrinol Metab* 87:213–221, 2002
32. Andersen L, Dinesen B, Jorgensen PN, Poulsen F, Roder ME: Enzyme immunoassay for intact human insulin in serum or plasma. *Clin Chem* 39:578–582, 1993
33. Pincus SM: Approximate entropy as a measure of system complexity. *Proc Natl Acad Sci U S A* 88:2297–2301, 1991
34. Schmitz O, Porksen N, Nyholm B, Skjaerbaek C, Butler PC, Veldhuis JD, Pincus SM: Disorderly and nonstationary insulin secretion in relatives of patients with NIDDM. *Am J Physiol* 272:E218–E226, 1997
35. Pincus SM, Hartman ML, Roelfsema F, Thorner MO, Veldhuis JD: Hormone pulsatility discrimination via coarse and short time sampling. *Am J Physiol* 277:E948–E957, 1999
36. Veldhuis JD, Pincus SM: Orderliness of hormone release patterns: a complementary measure to conventional pulsatile and circadian analyses. *Eur J Endocrinol* 138:358–362, 1998
37. Westermark P, Li ZC, Westermark GT, Leckstrom A, Steiner DF: Effects of beta cell granule components on human islet amyloid polypeptide fibril formation. *FEBS Lett* 379:203–206, 1996
38. Charge SB, de Koning EJ, Clark A: Effect of pH and insulin on fibrillogenesis of islet amyloid polypeptide in vitro. *Biochemistry (Mosc)* 34:14588–14593, 1995
39. Ohsawa H, Kanatsuka A, Yamaguchi T, Makino H, Yoshida S: Islet amyloid polypeptide inhibits glucose-stimulated insulin secretion from isolated rat pancreatic islets. *Biochem Biophys Res Commun* 160:961–967, 1989
40. Le Gurun S, Martin D, Formenton A, Maechler P, Caille D, Waeber G, Meda P, Haefliger JA: Connexin-36 contributes to control function of insulin-producing cells. *J Biol Chem* 278:37690–37697. Epub 32003 May 37622, 2003
41. Calabrese A, Zhang M, Serre-Beinier V, Caton D, Mas C, Satin LS, Meda P: Connexin 36 controls synchronization of Ca^{2+} oscillations and insulin secretion in MIN6 cells. *Diabetes* 52:417–424, 2003
42. Schmitz O, Porksen N, Juhl C, Veldhuis JD, Butler PC, Pincus SM: Disorderly insulin release processing in NIDDM assessed by approximate entropy (Abstract). *Diabetologia* 41 (Suppl. 1):S84, 1998